Elsevier Editorial System(tm) for
International Journal of Thermal Sciences
Manuscript Draft

Manuscript Number: THESCI-D-15-00725R2

Title: Boiling heat transfer and pressure drop of NH3/LiNO3 and NH3/(LiNO3+H2O) in a plate heat exchanger

Article Type: Research Paper

Keywords: flow boiling; plate heat exchanger; ammonia; lithium nitrate, absorption refrigeration

Corresponding Author: Prof. Mahmoud Bourouis, Ph.D.

Corresponding Author's Institution: Rovira i Virgili University

First Author: Francisco Táboas, PhD

Order of Authors: Francisco Táboas, PhD; Mahmoud Bourouis, Ph.D.; Manel Vallès, PhD

Abstract: This paper presents the experiments carried out to determine the flow boiling heat transfer coefficient and associated frictional pressure drop in a plate heat exchanger which uses the binary fluid mixture ammonia/lithium nitrate and the ternary fluid mixture ammonia/(lithium nitrate + water) with a water content in the absorbent of 20 % by weight. The effects on the flow boiling heat transfer coefficient and two phase frictional pressure drop are analysed with a heat flux range of 5 to 20 kW·m-2, a mass flux of 50 to 100 kg·m-2·s-1 and a mean vapour quality of 0 to 0.2.
The mass flux greatly influenced the flow boiling heat transfer coefficient, whereas the addition of water only produced a slight increase. The measurements taken experimentally indicated that the parameters with a pronounced effect on the frictional pressure drop were vapour quality followed by mass flux. Finally, the correlations proposed in Táboas et al. [1] used to predict the flow boiling heat transfer coefficient and frictional pressure drop were well in agreement with the experimental results.

*Manuscript
Click here to view linked References

Boiling heat transfer and pressure drop of $NH_3/LiNO_3$ and $NH_3/(LiNO_3+H_2O)$ in a plate heat exchanger

Francisco Táboas[b], Mahmoud Bourouis[a, 1], Manel Vallès[a]

[a] Department of Mechanical Engineering, Universitat Rovira i Virgili, Av. Països Catalans No. 26, 43007 Tarragona, Spain.

[b] Universidad de Córdoba, Campus de Rabanales, Edificio Leonardo da Vinci, 14014 Córdoba, Spain.

* *Corresponding Author (Email: mahmoud.bourouis@urv.cat; Phone: +34 977 55 86 13; Fax: +34 977 55 96 91)*

Keywords: flow boiling; plate heat exchanger; ammonia; lithium nitrate, absorption refrigeration

Highlights:

- Flow boiling heat transfer and frictional two-phase pressure drop for $NH_3/LiNO_3$ and $NH_3/(LiNO_3+H_2O)$ in a PHE are presented
- The effects of heat flux, mass flux and vapour quality on the flow boiling heat transfer and frictional pressure drop are analysed
- Mass flux has the most influence on the flow boiling heat transfer
- Those parameters with a pronounced effect on the frictional pressure drop are the vapour quality followed by the mass flux

Abstract

This paper presents the experiments carried out to determine the flow boiling heat transfer coefficient and associated frictional pressure drop in a plate heat exchanger which uses the binary fluid mixture ammonia/lithium nitrate and the ternary fluid mixture ammonia/(lithium nitrate + water) with a water content in the absorbent of 20 % by weight. The effects on the flow boiling heat transfer coefficient and two phase frictional pressure drop are analysed with a heat flux range of 5 to 20 $kW \cdot m^{-2}$, a mass flux of 50 to 100 $kg \cdot m^{-2} \cdot s^{-1}$ and a mean vapour quality of 0 to 0.2.

The mass flux greatly influenced the flow boiling heat transfer coefficient, whereas the addition of water only produced a slight increase. The measurements taken experimentally indicated that the parameters with a pronounced effect on the frictional pressure drop were vapour quality followed by mass flux. Finally, the correlations proposed in Táboas et al. [1] used to predict the flow boiling heat transfer coefficient and frictional pressure drop were well in agreement with the experimental results.

Nomenclature

A	Heat transfer area (m^2)
b	Amplitude of the plate (m)
Bo	Boiling number (-)
Cp	Heat capacity ($J \cdot kg^{-1} \cdot K^{-1}$)
D_h	Hydraulic diameter (m)
e	Plate thickness (m)
g	Gravitational acceleration ($m \cdot s^{-2}$)
G	Mass flux ($kg \cdot m^{-2} \cdot s^{-1}$)
h	Heat transfer coefficient ($W \cdot m^{-2} \cdot K^{-1}$)
H	Height of the plate (m)
k	Thermal conductivity ($W \cdot m^{-1} \cdot K^{-1}$)
Ke/V	Kinetic energy per unit of volume ($J \cdot m^{-3}$)
L	Flow length of the plate (m)
$LMTD$	Log mean temperature difference
m	Mass flow rate ($kg \cdot s^{-1}$)
Nu	Nusselt number
P	Pressure (bar)
Pr	Prandtl number
Q	Heat power (W)
R	Thermal resistance ($K \cdot W^{-1}$)
Re	Reynolds number
T	Temperature (K)
U	Global heat transfer coefficient ($W \cdot m^{-1} \cdot K^{-1}$)

u	Velocity ($m \cdot s^{-1}$)
V	Volume (m^{-3})
W	Width of the plate (m)
w	Liquid mass fraction
y	Vapour mass fraction
z	Total mass fraction

Greek symbols

β	Corrugation angle
Λ	Pitch (m)
ρ	Density ($kg \cdot m^{-3}$)
μ	Dynamic viscosity ($kg \cdot m^{-1} \cdot s^{-1}$)
φ	Chisholm two phase parameter
X_{LM}	Lockhart-Martinelli parameter

Subscripts

cb	Convective boiling
exp	Experimental
f	Friction
h	Hydraulic
in	Inlet
out	Outlet
L	Liquid
LO	Liquid overall
m	Homogenous

man	Manifold
mon	Momentum
nb	Nucleate boiling
ss	Solution side
steel	Stainless steel
T	Total
TP	Two phase
v	Vapour
w	Water
wall	Wall
ws	Water-side

1 Introduction

Nowadays most absorption heat pumps and chillers use water/lithium bromide or ammonia/water mixtures as working fluids. These working fluids have several drawbacks, such as crystallization, corrosion and low-pressure operating conditions for water/lithium bromide mixture. The refrigerant vapour leaving the generator needs to be rectified and the temperature required for the heat source should be higher for ammonia/water mixture. Other working fluids, such as ammonia/lithium nitrate (Gensch [2], Aggarwal and Agarwal [3], Infante Ferreira [4], Antonopoulos and Rogdakis [5], Kim and Machielsen [6]), have been studied for use as alternatives to overcome the aforementioned drawbacks.

The absorption refrigeration cycle can be operated at lower generator temperatures when using ammonia/lithium nitrate instead of ammonia/water and it is not necessary to

rectify the refrigerant vapour leaving the generator. The advantages of this working pair, therefore, are the simplicity of the cycle and the greater potential for using solar cooling or low grade temperature heat sources. However, the drawback with this working fluid is its high viscosity, which penalizes heat and mass transfer processes in the absorber and generator.

Infante Ferreira [4] compiled thermodynamic and thermophysical properties of the ammonia/lithium nitrate fluid mixture and proposed a series of correlations for their determination. These correlations were later used by several authors to carry out thermodynamic simulations of different absorption cycles such as single-effect (Antonopoulos and Rogdakis [5], Kim and Machielsen [6], Niebergall [7], Sun [8]), and double and half-effect ones (Bourouis et al. [9], Arzoz et al. [10] and Ayala et al. [11]).

Experimental data obtained with absorption cooling prototypes designed initially to operate with the ammonia/water working pair (Ayala et al. [12], Infante Ferreira [13], Heard [14]) and loaded with the ammonia/lithium nitrate working pair showed poor performance results. The authors of these experimental studies concluded that the main reason for the poor performance lay in the absorber and was due to the high viscosity of the fluid mixture compared with that of the ammonia/water mixture. High viscosity reduces the cycle performance predicted by the thermodynamic models. This decrease in the cycle performance is more pronounced at low temperatures of cooling-water due to the fact that the viscosity of the working fluid in the absorber increases drastically.

Ehmke and Renz [15], and Bokelmann et al. [16] proposed the addition of water to the binary mixture ammonia/lithium nitrate used in absorption heat pumps. Later, Reiner and Zaltash [17] proposed the use of the ternary mixture for GAX systems as an alternative to using ammonia/water systems.

Ehmke and Renz [15] studied the effect of adding water on the solubility and viscosity of the ternary mixture and suggested an optimal mass fraction of water between 0.20 and 0.25 in the absorbent mixture (lithium nitrate + water). These authors also determined and correlated data for the density and vapour pressure of the mixture at 0.25 of water mass fraction in the absorbent. Bokelmann et al. [16] carried out an experimental study dealing with the performance of an absorption heat pump working with the ternary fluid mixture ammonia/(lithium nitrate + water). The data were reported by Manago [18] in a study on new mixtures for absorption heat pumps for the Heat Pump Program of The International Energy Agency. Reiner and Zaltash [17] measured the densities and viscosities of the ternary mixture with an ammonia mass fraction of 0.04 and a water mass fraction of 0.605, which are the typical values for GAX systems.

In 1989, Bothe [19] published a comparative study carried out with ammonia/water and ammonia/(lithium nitrate + water) as working fluids for heat pumping applications. The author reported a significant improvement in COP using the ternary mixture compared to using the binary mixture.

Libotean et al. [20] obtained vapour pressure equilibrium data and Libotean et al. [21] measured viscosities, densities and heat capacities for the ammonia/lithium nitrate and ammonia/(lithium nitrate + water) mixtures. Linke [22], and Eysseltova and Orlova [23], published experimental data regarding the solubility of the binary and ternary mixtures. According to this data, the addition of a small amount of water improves the solubility of the mixture. Recently, Cuenca et al. [29] presented new experimental data on thermal conductivity for the ammonia/lithium nitrate and ammonia/(lithium nitrate + water) mixtures.

Regarding the flow boiling heat transfer coefficient and pressure drop of these mixtures, Rivera and Best [24] published experimental data on flow boiling in a vertical tube with mass fluxes of 7.4 and 13.7 $kg \cdot m^{-2} \cdot s$ and a heat flux of between 11.8 and 16.4 $kW \cdot m^{-2}$. The experimental local heat transfer coefficients were in the range of 1.3-4.0 $kW \cdot m^{-2} \cdot K^{-1}$. The authors reported that both the forced convective and nucleate boiling mechanisms were significant and they proposed a heat transfer coefficient correlation based on their experimental data.

Zacarías et al. [25] published data on the flow boiling heat transfer coefficient in plate heat exchangers with the mixture ammonia/lithium nitrate. The data was obtained with a maximum vapour quality generation of 0.03 and high subcooling of the solution entering the heat exchanger. The solution flow rate was varied between 0.041 and 0.083 $kg \cdot s^{-1}$. In the flow boiling region, the heat transfer coefficient ranged from 0.6 to 1.1 $kW \cdot m^{-2}\ K^{-1}$. The authors concluded from the experimental results, that nucleate boiling appeared to be the dominant factor.

Regarding the boiling of the ammonia/(lithium nitrate + water) fluid mixture, Sathyabhama and Ashok Babu [26] investigated the nucleate pool boiling heat transfer coefficient applying an operating pressure of 4 to 8 bar, an ammonia mass fraction ranging from 0 to 0.3 and different heat fluxes. The lithium nitrate concentration in the solution was chosen from the range of 10-50% of mass ratio of lithium nitrate in pure water. The effects of the concentration, heat flux, and pressure on the boiling heat transfer coefficient were analysed. The authors concluded that the heat transfer coefficient decreases with an increase in the ammonia mass fraction, increases with the addition of lithium nitrate and increases with a rise in heat flux and pressure. To the knowledge of the authors, there is currently no data available on flow boiling of the ammonia/(lithium nitrate + water) fluid mixture.

The objective of the present work is to contribute to the technological development of brazed plate heat exchangers (BPHEs) as desorbers for ammonia based absorption refrigeration systems. For this purpose, the flow boiling heat transfer coefficient and associated frictional pressure drop in a plate heat exchanger were measured for the binary ammonia/lithium nitrate and ternary ammonia/(lithium nitrate + water) fluid mixtures. The experimental results were analysed whilst varying mass flux, heat flux, vapour quality, pressure and mixture concentration.

2 Experimental set-up

Figure 1 shows a schematic diagram of the generator test bench, which consists of a solution circuit and three auxiliary circuits. The pre-evaporator circuit provides the desired vapour quality at the inlet of the test section. The heating circuit provides the heating for the test section and allows the heat flux to be fixed. The condensation circuit condenses the ammonia vapour which will be returned to the solution tank in order to regenerate the solution to the initial conditions.

The solution stored in the solution tank is pumped by the recirculation pump from the bottom through the pre-evaporator, where it is preheated to establish the required vapour quality at the generator inlet. Subsequently, the solution enters the plate heat exchanger (generator). The resulting two-phase flow at the outlet of the generator enters the solution tank and from the top of it the ammonia vapour is sent to the condenser where it condenses and is returned back to the solution tank to start the cycle again.

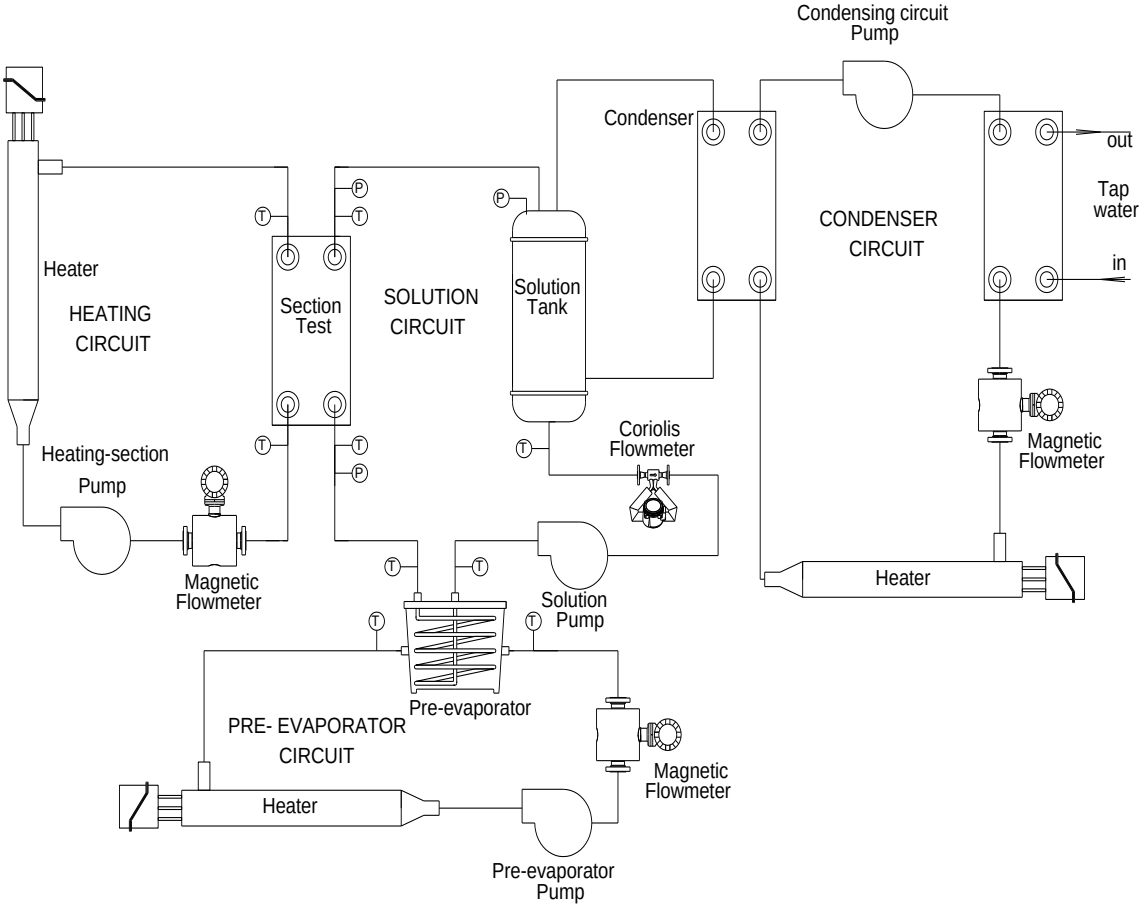

Figure 1. Schematic diagram of the experimental test bench

The solution and water temperatures of the auxiliary circuits were measured with Pt-100 sensors located at the points indicated in Figure 1. The flow rate and concentration of the solution entering the test section were determined using a Coriolis flowmeter. The water flow rates in the auxiliary circuits were measured by magnetic flowmeters. The pressure was measured by two pressure sensors located at the inlet and outlet of the plate heat exchanger (test section). More details about the experimental set-up and its components can be found in Táboas et al. [1].

The section test consists of a plate heat exchanger manufactured by Alfa Laval, NB51, with a chevron corrugation angle of 30 degrees to the horizontal and a plate thickness of

0.4 mm. The heat exchanger consists of four plates forming three channels. The solution circulates through the central channel while the hot water circulates through the side channels. A channel 100 mm wide was used to calculate the flow area. Figure 2 shows the main parameters of the plate heat exchanger.

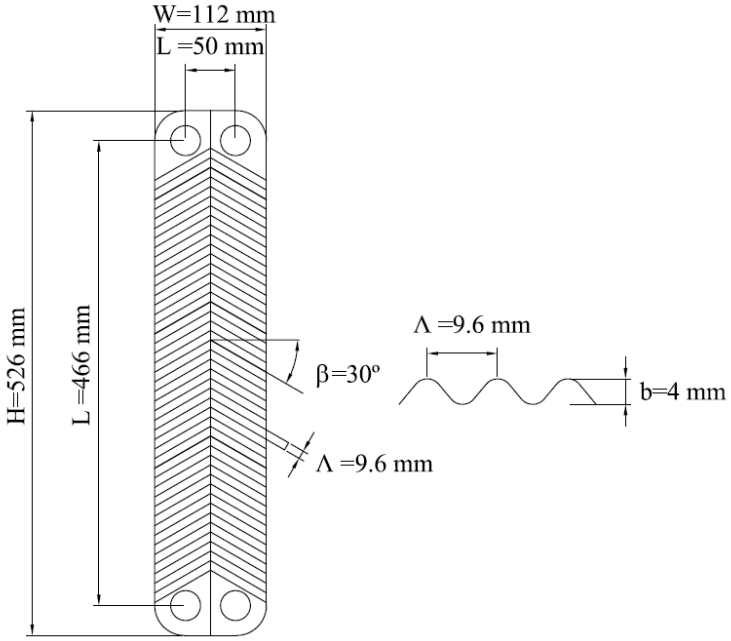

Figure 2. Main parameters of the plate heat exchanger

3 Methodology

The design of the test bench allows for flow boiling experiments to be carried out varying the following operating parameters: solution mass flow rate, solution inlet temperature, heating water inlet temperature, solution inlet concentration, and system pressure. In each experiment, once a steady-state regime was reached, all operating conditions were registered and stored for about 25 minutes. The parameters characterizing the generator behaviour were calculated as reported in the following sections.

3.1 Properties of the working fluid

Vapour-liquid equilibrium of the ammonia/lithium nitrate and ammonia/(lithium nitrate + water) fluid mixtures was calculated using the correlations reported by Libotean et al. [21]. The densities and viscosities of these fluid mixtures were calculated by the correlations of Libotean et al. [20].

The liquid enthalpies of both ammonia/lithium nitrate and ammonia/(lithium nitrate + water) fluid mixtures were obtained with the Haltenberger method [27] employed by McNeely [28] for the conventional working pair water/lithium bromide. This method was developed to obtain the liquid enthalpy of binary fluid mixtures in which only one component is volatile. In the case of the ternary fluid mixture, the procedure was the same, taking into account that the water content in the vapour phase was insignificant. The enthalpy reference value for ammonia is 0 kJ/kg at 0ºC, and the reference state for the ammonia/lithium nitrate and ammonia/(lithium nitrate + water) fluid mixtures was obtained with an ammonia mass fraction of 0.5 at 0ºC. The thermal conductivity of both fluid mixtures was determined from the data reported by Cuenca et al. [29].

3.2 Single-phase heat transfer coefficient and pressure drop

The water-side heat transfer coefficient (h_{ws}) was determined by carrying out preliminary tests using water in both the hot and cold sides. The thermal load of the heat exchanger was obtained as the average value of the heat transfer rate calculated on the hot and cold sides (Eqs. (1-3)).

$$Q_{ws} = m_{ws} \cdot Cp_{ws} \cdot \left(T_{ws,out} - T_{ws,in} \right) \quad (1)$$

$$Q_{ss} = m_{ss} \cdot Cp_{ss} \cdot \left(T_{ss,out} - T_{ss,in}\right) \quad (2)$$

$$Q_{mean} = \frac{Q_{ss} + Q_{ws}}{2} \quad (3)$$

Once the thermal load is obtained, the experimental global heat transfer coefficient can be calculated as follows:

$$U_{\exp} = \frac{Q_{mean}}{A \cdot LMTD} \quad (4)$$

Where LMTD is the logarithmic mean temperature difference involving inlet and outlet temperatures in the generator (Eq. (5)):

$$LMTD = \frac{(T_{ws,in} - T_{ss,out}) - (T_{ws,out} - T_{ss,int})}{Ln\left(\frac{(T_{ws,in} - T_{ss,out})}{T_{ws,out} - T_{ss,int}}\right)} \quad (5)$$

Eq. (4) is compared with the overall heat transfer coefficient expressed by Eq. (6) that combines the different thermal resistances between the solution and the coolant streams.

$$\frac{1}{U} = \frac{1}{h_{ws}} + \frac{1}{h_{ss}} + \frac{e}{k_{steel}} \quad (6)$$

Where the single-phase heat transfer coefficient, expressed by the correlation of Eq. (7), was obtained by a least square adjustment between U_{exp} and U. The expression is valid for the turbulent regime (Re: 690 – 3100) with a coefficient of determination R^2=0.998.

$$h = 0.577 \frac{k}{D_h} Re^{0.634} Pr^{1/3} \quad (7)$$

The single-phase friction pressure drop was calculated by subtracting the static and manifold pressure drops from the total pressure drop, as shown in Eq. (8):

$$\Delta P_f = \Delta P_{total} - \Delta P_{static} - \Delta P_{man} \quad (8)$$

The static pressure drop was calculated by Eq. (9):

$$\Delta P_{static} = g \cdot \rho_{mean} \cdot L \quad (9)$$

Where ρ_{mean} is the density calculated at the average temperature between the inlet and outlet of the generator.

The pressure drop at the manifolds was estimated using the correlation reported by Shah and Focke [30], Eq. (10):

$$\Delta P_{man} = 1.5 \cdot \left(\frac{\rho \cdot u^2}{2} \right) \quad (10)$$

Finally, the Fanning friction factor was calculated using equation Eq. (11):

$$f = \frac{\Delta P \cdot D_h \cdot \rho}{2 \cdot G^2 \cdot L} \quad (11)$$

According to our experimental data, the correlation for the single-phase flow friction factor is given by Eq. (12) with R^2=0.992. This equation was obtained for the Reynolds number in the range 375-2500.

$$f = 4.778 \cdot \mathrm{Re}^{-0.118} \quad (12)$$

3.3 Flow boiling heat transfer coefficient

The approach used to calculate the flow boiling heat transfer coefficient on the solution side is described below. Firstly, the heat transfer rate was calculated from Eq. (13). The experimental overall heat transfer coefficient and the logarithmic mean temperature difference (*LMTD)* were calculated as in single-phase experiments by Eqs. (14) and (15):

$$Q_{ws} = m_{ws} \cdot Cp_{ws} \cdot \left(T_{ws,out} - T_{ws,in} \right) \quad (13)$$

$$U = \frac{Q_{ws}}{A \cdot LMTD} \quad (14)$$

$$LMTD = \frac{\left(T_{ws,in} - T_{ss,out} \right) - \left(T_{ws,out} - T_{ss,in} \right)}{Ln\left(\frac{T_{ws,in} - T_{ss,out}}{T_{ws,out} - T_{ss,in}} \right)} \quad (15)$$

Finally, the flow boiling heat transfer coefficient was calculated from Eq. (16), while h_{ws} was computed with Eq. (7):

$$\frac{1}{h_{TP}} = \frac{1}{U} - \left(\frac{1}{h_{ws}} + \frac{e}{k_{steel}} \right) \quad (16)$$

The global ammonia mass fraction of the solution was obtained using a Coriolis flowmeter to measure the density and temperature and by taking into consideration the density correlations from Libotean et al. [20]. The ammonia liquid mass fraction at the inlet and outlet of the heat exchanger was obtained by measuring the pressure and temperature and using the vapour-liquid equilibrium data of Libotean et al. [21]. Then the vapour quality of the mixture at the inlet and outlet of the heat exchanger was obtained by applying the liquid and global ammonia mass fraction, Eqs. (17)-(19):

$$m_L + m_V = m_T \quad (17)$$

$$m_L \cdot w + m_V = m_T \cdot z \quad (18)$$

$$x = \frac{m_V}{m_T} \quad (19)$$

The mean vapour quality was then assumed to be the average of the numerical values calculated at the inlet and outlet of the generator (Eq. (20)).

$$x_{mean} = \frac{x_{in} + x_{out}}{2} \quad (20)$$

3.4 Flow boiling two-phase pressure drop

The total two-phase pressure drop in the plate heat exchanger is the sum of the frictional pressure drop, the static pressure drop, the momentum pressure drop, and the pressure drop produced by manifolds and ports.

323 The total pressure drop was determined experimentally using pressure transducers
324 located at the entrance and exit of the solution in the plate heat exchanger. The frictional
325 pressure drop, $\Delta P_{f,TP}$, associated with the two-phase solution flowing through the
326 channel of the heat exchanger was obtained by Eq. (21):

327 $$\Delta P_{f,TP} = \Delta P_{total} - \Delta P_{static} - \Delta P_{mon} - \Delta P_{man} \quad (21)$$

328 The static pressure drop ΔP_{static} was determined as follows:

329 $$\Delta P_{static} = g \cdot \rho_m \cdot L \quad (22)$$

330 where the average density ρ_m is obtained from the homogeneous model for two-phase
331 flow (Eq. (23)):

332 $$\rho_m = \left[\frac{x_{mean}}{\rho_V} + \frac{(1-x_{mean})}{\rho_L}\right]^{-1} \quad (23)$$

333 The momentum pressure drop was estimated as follows:

334 $$\Delta P_{mon} = G^2 \cdot \left(\frac{1}{\rho_V} - \frac{1}{\rho_L}\right) \cdot \Delta x \quad (24)$$

335 The pressure drop resulting from manifolds and ports can be estimated using the
336 correlation reported by Shah and Focke [30], Eq. (25):

337 $$\Delta P_{man} \cong 1.5 \cdot \left(\frac{G^2}{2 \cdot \rho_m}\right) \quad (25)$$

338 Finally, after obtaining the value of $\Delta P_{f,TP}$, the Fanning friction factor for a two-phase
339 flow can be calculated as follows:

340 $$f_{TP} = \frac{\Delta P_{f,TP} \cdot D_h \cdot \rho_m}{2 \cdot G^2 \cdot L} \quad (26)$$

3.5 Uncertainty of the measured and calculated parameters

The approach used for determining the propagation of the uncertainty for the indirect variables was that proposed in the Technical Note 1297 of the National Institute of Standards and Technology (NIST) (Taylor and Kuyyat 1994). The EES (Engineering Equation Solver) software was used to perform the error analysis. Table 1 shows the accuracy of the variables measured and the combined uncertainty for the most relevant parameters calculated.

Table 1.Accuracy of measured variables and combined uncertainty of the calculated parameters

Measured variable	Accuracy
Temperature, T (ºC)	± 0.1
Pressure, P (bar)	± 0.016
Water flow rate, m_w (L/h)	± 0.24
Solution flow rate, m_s (%)	± 0.1
Solution density, ρ (kg/m^3)	± 0.5
Calculated parameter	Combined uncertainty
Vapour Quality	± 0.0050-0.012
Flow boiling heat transfer coefficient, h (%)	±3.32-14.51
Friction factor, f (%)	±5.36-34.5

4 Results and discussion

Experimental results which were obtained on the generator test bench using the binary ammonia/lithium nitrate and ternary ammonia/(lithium nitrate + water) fluid mixtures are examined in this section. Operating conditions selected for temperature, pressure, solution mass flux, heat flux and concentration are summarized in Table 2. The effects of solution mass flux and heat flux on the experimental flow boiling heat transfer coefficient and associated frictional pressure drop are presented below and discussed with the variation of the mean vapour quality in the test section.

Table 2. Operating conditions

Parameters	***Range***
Heat flux, ($kW \cdot m^{-2}$)	5.0, 10.0 and 20.0
Solution mass flux, ($kg \cdot s^{-1}.m^{-2}$)	50 – 100
Ammonia mass fraction of the solution at the generator inlet (binary mixture)	0.49-0.54
Ammonia mass fraction of the solution at the generator inlet (ternary mixture)	0.42-0.46
Water content in the absorbent for the ternary mixture, (mass fraction)	0.20
Mean generator pressure, (bar)	12-15
Mean vapour quality, (kg vapour / (kg solution +kg vapour))	0 – 0.16

Moreover, the experimental values of the flow boiling heat transfer coefficient obtained with the binary mixture ammonia/lithium nitrate have been compared with those reported by Zacarías et al. [25] for the desorption process of the same fluid mixture in a plate heat exchanger which operated at the following experimental operating conditions: mass flux ranging from 10 to 20.2 $kg \cdot m^{-1} \cdot s^{-2}$, pressure from 9.78 to 16.06 bar, ammonia mass fraction from 0.452 to 0.462 and heat flux from 1.203 to 4.618 $kW \cdot m^{-2}$.

4.1 Two-phase Pressure drop

The total pressure drop for the ammonia/ lithium nitrate and ammonia / (lithium nitrate + water) fluid mixtures was measured on the test bench, and the frictional pressure drop was determined as described in section 3.4.

Figure 3 shows the experimental frictional pressure drop in the PHE as a function of the mean vapour quality for the binary and ternary fluid mixtures. Heat fluxes were imposed at 5, 10 and 20 $kW \cdot m^{-2}$, operating pressure at between 12 and 15 bar and solution mass flux between 50 and 100 $kg \cdot m^{-2} \cdot s^{-1}$. In the case of the ammonia/lithium nitrate fluid mixture, the ammonia concentration ranged from 0.49 to 0.54, while in the case of the ammonia/(lithium nitrate + water) fluid mixture the ammonia concentration was between 0.42 and 0.46. The water content in the absorbent remained at 20%. The results are in concordance with the results reported by other authors, Hsieh and Lin [31], Yan and Lin [33], Claesson [33], Táboas et al. [1], who concluded that vapour quality followed by mass flux have the most significant effect on frictional pressure drop. For the selected experimental conditions, it is noteworthy that operating pressure, ammonia mass fraction and heat flux have no significant effect on frictional pressure drop.

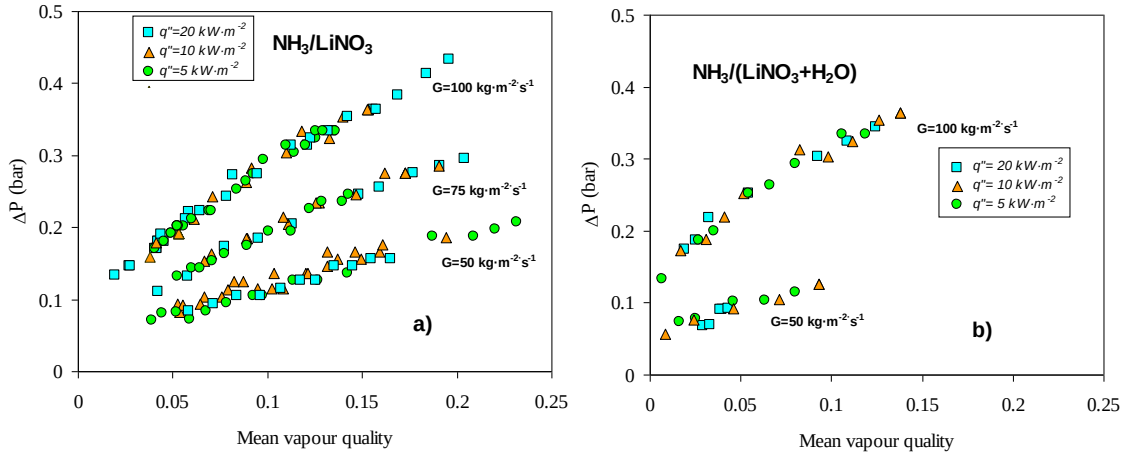

Figure 3. Two-phase frictional pressure drop versus mean vapour quality at different mass fluxes and heat fluxes for: (a) $NH_3/LiNO_3$ and (b) $NH_3/(LiNO_3+H_2O)$

Figure 4 shows the friction factor versus mean vapour quality at solution mass flux of 50, 75 and 100 $kg \cdot s^{-1} \cdot m^{-2}$. The results indicate that the friction factor significantly decreases when the solution mass flux is increased. Furthermore, the friction factor decreases significantly with an increase in mean vapour quality for vapour qualities lower than 0.15.

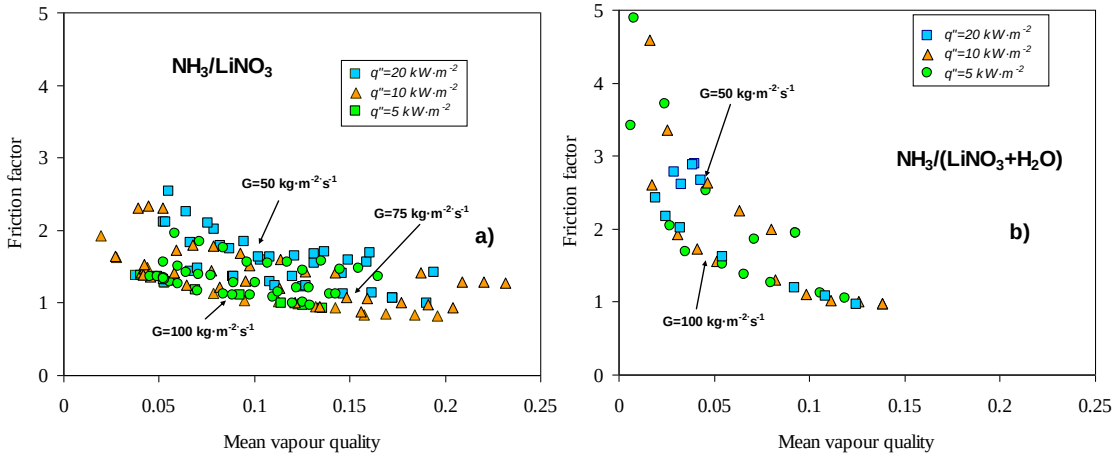

Figure 4. Two-phase friction factor versus mean vapour quality at different mass fluxes and heat fluxes for: (a) $NH_3/LiNO_3$ and (b) $NH_3/(LiNO_3+H_2O)$

4.2 Flow boiling heat transfer

4.2.1 Flow boiling of ammonia/lithium nitrate fluid mixture

Figure 5 shows the influence of mean vapour quality on the flow boiling heat transfer coefficient when using the ammonia/lithium nitrate fluid mixture at different mass fluxes and three heat fluxes, namely, (a) 5 $kW \cdot m^{-2}$, (b) 10 $kW \cdot m^{-2}$ and (c) 20 $kW \cdot m^{-2}$. The experiments were carried out with an ammonia mass fraction of 0.50 and at an average operating pressure of 15 bar.

The results show that the flow boiling heat transfer coefficient is greatly dependent on the solution mass flux at all selected operating conditions. This indicates the importance of the effects of convective boiling in the experimental data. The results are well in agreement with the data of Táboas et al. [1] obtained for ammonia/water and the same plate heat exchanger (PHE) and also with the data reported by Yan and Lin [32] for R-134a in a PHE.

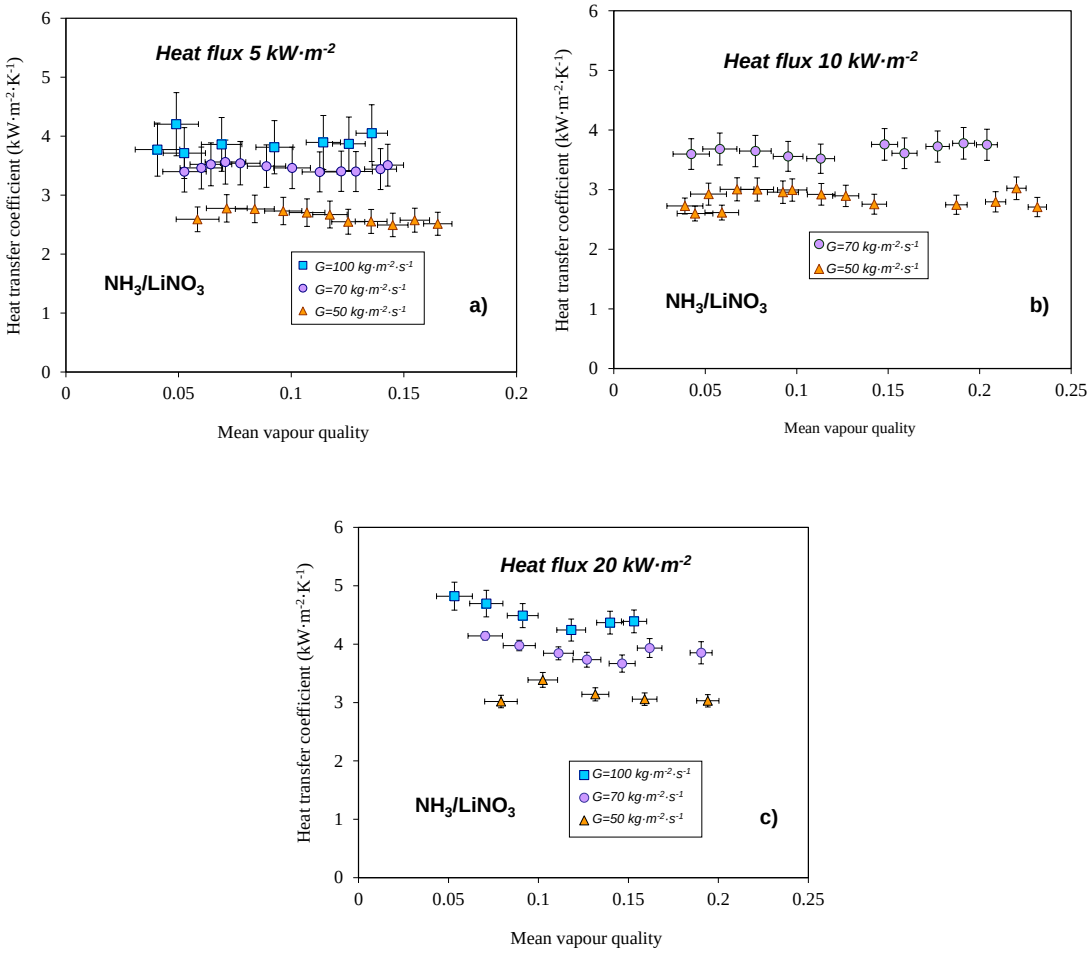

Figure 5. Flow boiling heat transfer coefficient versus mean vapour quality for $NH_3/LiNO_3$ at different mass fluxes and heat flux of: (a) 5 kW·m^{-2}, (b) 10 kW·m^{-2} and (c) 20 kW·m^{-2}

It is noteworthy that the experimental results presented in this work, like those of Táboas et al. [1] and Yan and Lin [32], were obtained with a mass flux considerably higher than that used by other authors, who suggested that flow boiling heat transfer in PHE was dominated by nucleation effects (Hsieh and Lin [31], Longo and Gasparella [34], Palm and Claesson [35], Zacarías et al. [25]).

Figure 6 shows the influence of heat flux on the flow boiling coefficient for $NH_3/LiNO_3$ at three values of mass flux, namely, (a) 100 $kg \cdot m^{-2}$, (b) 75 $kg \cdot m^{-2}$ and (c) 50 $kg \cdot m^{-2}s$. As is observed, the heat flux has a limited effect compared to that of the mass flux. In the case of a fluid mixture, the presence of the second component in the liquid phase causes a resistance to the boiling process which results in the boiling heat transfer coefficient being less dependent on heat flux. Nevertheless, the experimental works available in the literature on flow boiling heat transfer coefficient in PHEs with pure fluids, which report correlations fitted to their own data (Hsieh and Lin [31], Yan and Lin [32], Han et al. [36], Djordjevic and Kabelac [37]), always show a lower heat flux exponent than the typical value of 0.7 used for smooth tubes.

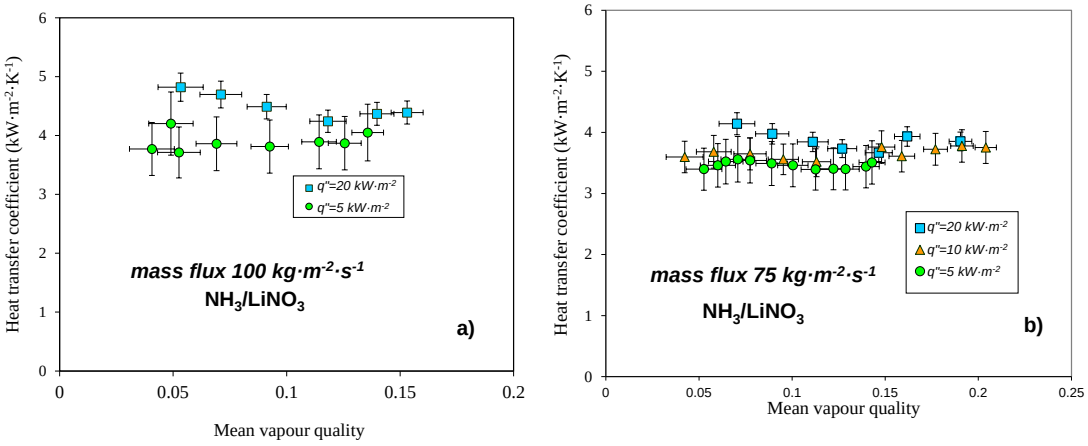

433

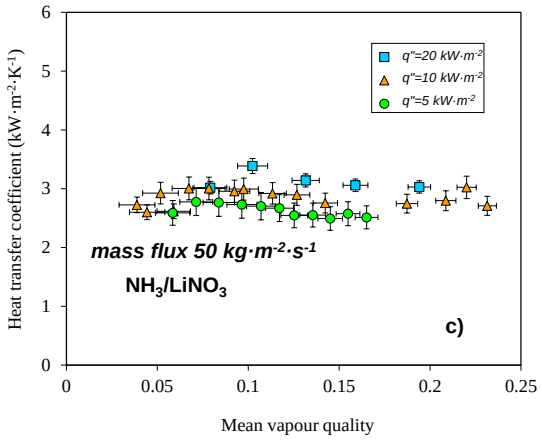

434

435 **Figure 6. Flow boiling heat transfer coefficient versus mean vapour quality for $NH_3/LiNO_3$ at**
436 **different heat fluxes and mass flux of: (a) 100 kg·m^{-2}s^{-1}, (b) 75 kg·m^{-2}s^{-1} and (c) 50 kg·m^{-2}s^{-1}**

437

438 Therefore, the flow boiling process of ammonia/lithium nitrate in the plate heat
439 exchanger tested comprises both convective and nucleate effects. Convective effects are
440 dominant for low heat fluxes and high solution mass fluxes, nucleate effects are present
441 for low solution mass fluxes. It is also worthwhile mentioning that even in the zone of
442 apparent nucleation (high heat flux and low mass flux) the mass flux clearly has an
443 influence on the flow boiling heat transfer coefficient.

444 The heat transfer coefficients reported by Zacarías et al. [25] with $NH_3/LiNO_3$ and a
445 similar plate heat exchanger, are considerably lower than those in the data obtained in
446 the present work. However, it is not possible to make a direct quantitative comparison

because, although the authors present experimental results with a heat flux close to 5 kW/m^2, the experiments were performed with a maximum mass flux of 19.8 kg·m^{-2}s^{-1} and a maximum vapour quality of 3%.

4.2.2 Comparison of the ammonia/lithium nitrate with other ammonia based fluid mixtures

Figure 7 shows a comparison of the flow boiling heat transfer coefficient between ammonia/lithium nitrate and ammonia/(lithium nitrate + water) fluid mixtures at: (a) mass flux of 100 kg·m^{-2}·s^{-1} and heat flux of 20 kW·m^{-2} and (b) mass flux of 50 kg·m^{-2}·s^{-1} and heat flux of 10 kW·m^{-2}. It is seen that the flow boiling heat transfer coefficient is somewhat higher in the case of the ternary fluid mixture. This is attributed to the lower viscosity and higher thermal conductivity of the ternary fluid mixture which improve the boiling coefficient.

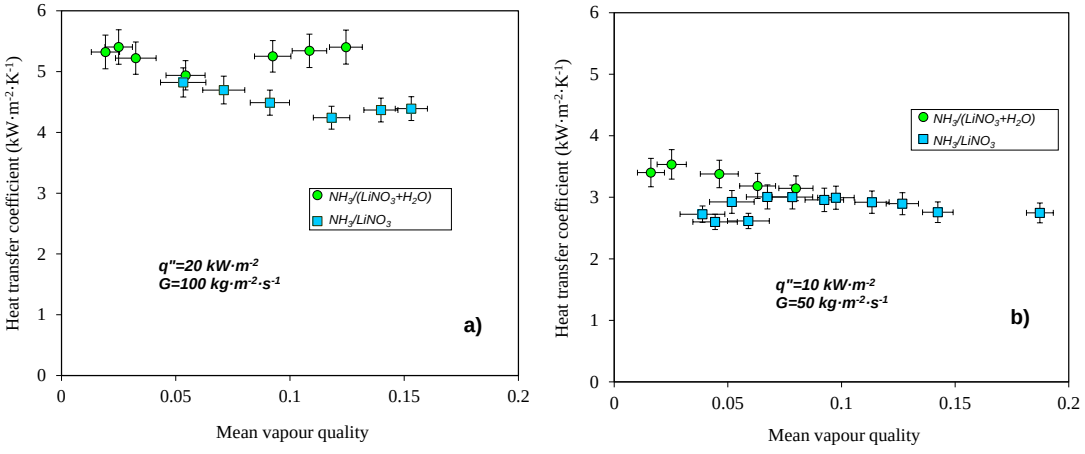

Figure 7. Comparison between the flow boiling heat transfer coefficients of the binary and ternary fluid mixtures at: (a) heat flux of 20 kW·m^{-2} and mass flux of 100 kg·m^{-2}·s^{-1}; (b) heat flux of 10 kW·m^{-2} and mass flux of 50 kg·m^{-2}·s^{-1}

Figure 8 compares the flow boiling heat transfer coefficients obtained in the present work at mass fluxes of 100 and 75 $kg \cdot m^{-2}\ s^{-1}$ and a heat flux of 20 $kW \cdot m^{-2}$, with those obtained by Táboas et al. [1] for ammonia/water fluid mixture at similar operating conditions. The experimental data for ammonia/water was obtained with a mass fraction of 0.42, an operating pressure of 15 bar, mass fluxes of 100, 70 $kg \cdot m^{-2} \cdot s^{-1}$ and a heat flux of 20 $kW \cdot m^{-2}$. The flow boiling heat transfer coefficients obtained in the present work are at least 35% lower than those presented by Táboas et al. [1]. Again, the higher viscosity and the lower thermal conductivity of the ammonia/lithium nitrate fluid mixture are considered responsible for the lower values of the flow boiling heat transfer coefficient obtained.

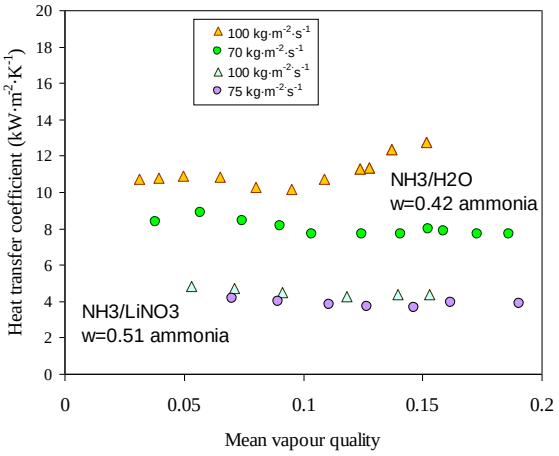

Figure 8. Comparison of the flow boiling heat transfer coefficient with $NH_3/LiNO_3$ fluid mixture (present work) with data obtained by Táboas et al. [1] for NH_3/H_2O

Besides, Táboas et al. [1] who carried out their work in the same experimental set-up using ammonia/water as a working pair, at mass fluxes higher than 70 $kg \cdot m^{-2} \cdot s^{-1}$ observed that the flow boiling heat transfer coefficient is not dependent on the heat flux but is clearly dependent on the vapour quality. This region of operating conditions was

considered a purely convective region, since heat flux has no effect on the boiling heat transfer coefficient while mass flux and vapour quality have. The experimental data of the present work do not show the pure convective boiling region that Táboas et al. [1] observed in their data at high mass fluxes. The higher viscosity of the binary fluid mixture used in this study, reduces the turbulence in the heat exchanger at the same mass flux and could delay the presence of pure convective boiling effects in the heat exchanger.

4.3 Modelling of two-phase frictional pressure drop and flow boiling heat transfer coefficient

4.3.1 Modelling of two-phase frictional pressure drop in the plate heat exchanger

From the single-phase friction factor calculated with Eq. (26) and developed in section 3.4, the two-phase frictional pressure drop was correlated using the Lockhart-Martinelli approach and the Chisholm parameter C (Eqs. (27)-(29)).

$$\varphi_L^2 = \frac{\left(\frac{\Delta P}{\Delta L}\right)_{TP}}{\left(\frac{\Delta P}{\Delta L}\right)_L} \quad (27)$$

$$\varphi_L^2 = 1 + \frac{C}{X_{LM}} + \frac{1}{X_{LM}^2} \quad (28)$$

$$X_{LM}^2 = \frac{\left(\Delta P/\Delta L\right)_L}{\left(\Delta P/\Delta L\right)_V} \quad (29)$$

According to Táboas et al. [38], a value equal to 3 was obtained for the parameter C in experiments performed with ammonia/water fluid mixture and the plate heat exchanger employed later in the present work. Figure 9 shows the results obtained using the same

value of parameter C and, as seen, this same value also correlates reasonably well with the two-phase frictional pressure drop. Figure 9a shows the comparison between the measured and the predicted two-phase frictional pressure drop for the two fluid mixtures studied in the present work, namely ammonia/lithium nitrate and ammonia/(lithium nitrate + water). Figure 9b incorporates the set of data obtained in the present work and that obtained by Táboas et al. [38] for ammonia/water.

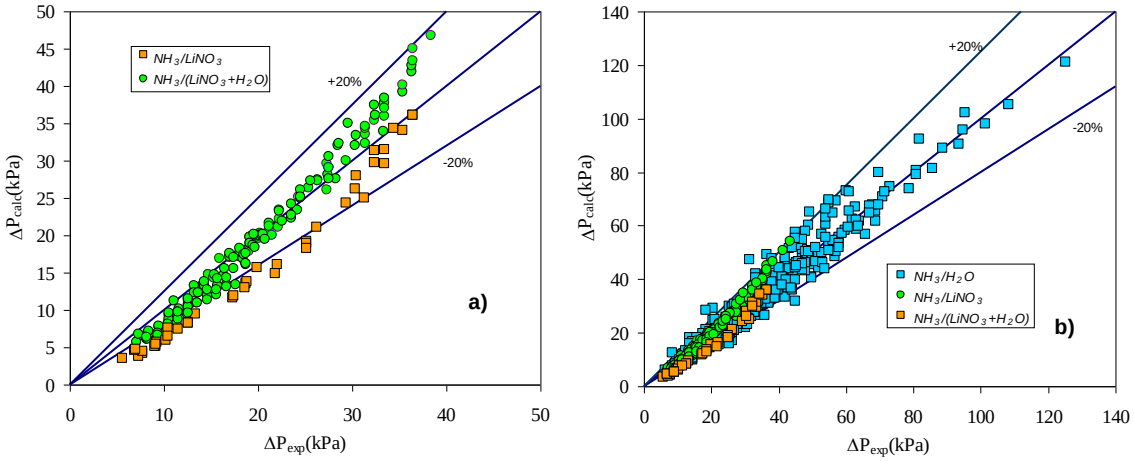

Figure 9. Two-phase frictional pressure drop for: (a) binary and ternary fluid mixtures, (b) binary, ternary and NH_3/H_2O fluid mixtures

The experimental two-phase frictional pressure drop values obtained for the ammonia/lithium nitrate fluid mixture have also been compared with the experimental data reported by Zacarías et al. [25] who presented the two-phase frictional pressure drop against the kinetic energy per unit volume computed by the homogeneous model, Eq. (30).

$$\frac{KE}{V} = \frac{G^2}{2 \cdot \rho_m} \tag{30}$$

Figure 10 shows that the slopes of both sets of data and operating conditions are different.

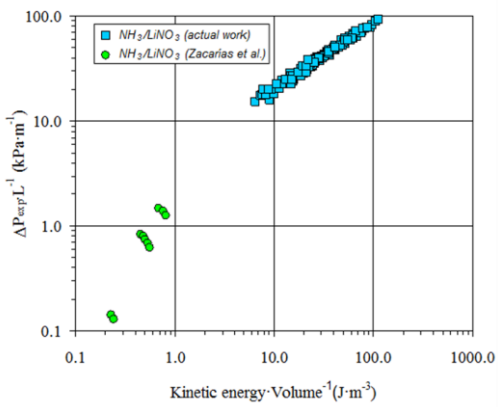

Figure 10. Frictional pressure drop per unit length versus the kinetic energy per unit volume. Comparison between the present work and Zacarías et al. [25].

4.3.2 Modelling of the flow boiling heat transfer in plate heat exchangers.

Táboas et al. [38] showed that the flow boiling heat transfer coefficient for the ammonia/water fluid mixture could be calculated by the following set of equations:

$$If\ u_V < -111.88 \cdot u_L + 11.848 \qquad h_{TP} = h_{nb} = 5 \cdot Bo^{0.15} \cdot h_{LO}$$

$$If\ u_V > -111.88 \cdot u_L + 11.848 \quad h_{TP}\ higher\ of \begin{Bmatrix} h_{nb} = 5 \cdot Bo^{0.15} \cdot h_{LO} \\ h_{cb} = \left(1 + \frac{3}{X_{LM}} + \frac{1}{X^2}\right)^{0.2} \cdot h_{LO} \end{Bmatrix} \quad (31)$$

These relationships depend on easy-to-calculate properties of binary fluid mixtures used in absorption refrigeration systems. In addition, the convective enhancement factor was characterized by the Chisholm equation, so the convective boiling term can be calculated from the experimental data of a two-phase frictional pressure drop, which makes use of the single-phase friction factor equation.

Figure 11 shows the predictions of the flow boiling heat transfer coefficient for the ammonia/lithium nitrate fluid mixture using the Eq. (31) proposed by Táboas et al. [38]

for ammonia/water mixtures in plate heat exchangers. The predictions are presented at different mass fluxes and three values of heat flux, namely, 5, 10 and 20 kW·m^{-2}. As observed, the equations predict the trend and data reasonably well.

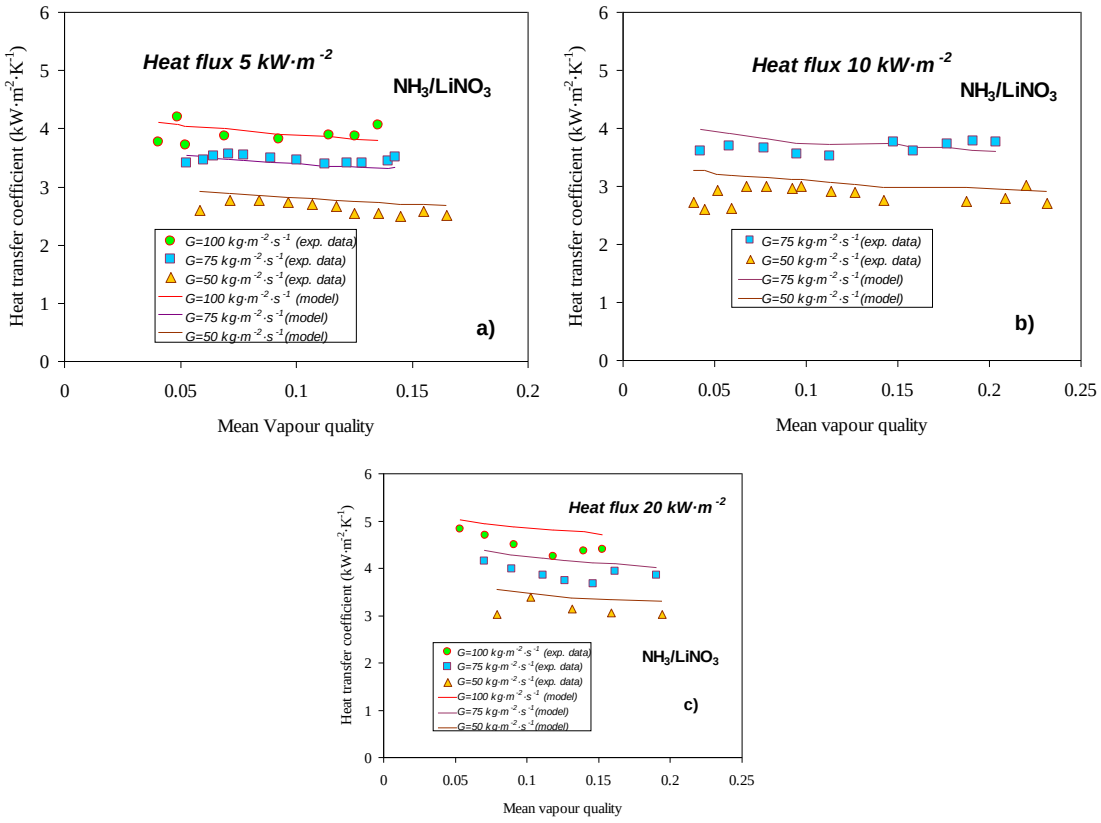

Figure 11: Comparison between the values predicted by the correlation of Táboas et al. [38] and experimental data of the flow boiling heat transfer coefficient for $NH_3/LiNO_3$ at different mass fluxes and heat flux of: (a) 5 kW·m^{-2} , (b) 10 kW·m^{-2} and (c) 20 kW·m^{-2}

Figure 12 shows a similar comparison to Figure 11 for the binary fluid mixture $NH_3/LiNO_3$ but at different heat fluxes and three values of mass flux, namely, 50, 75 and 100 kg·m^{-2}·s^{-1}. As shown in this figure, the exponent chosen for the boiling number was able to predict the heat transfer coefficient trend reasonably well.

554

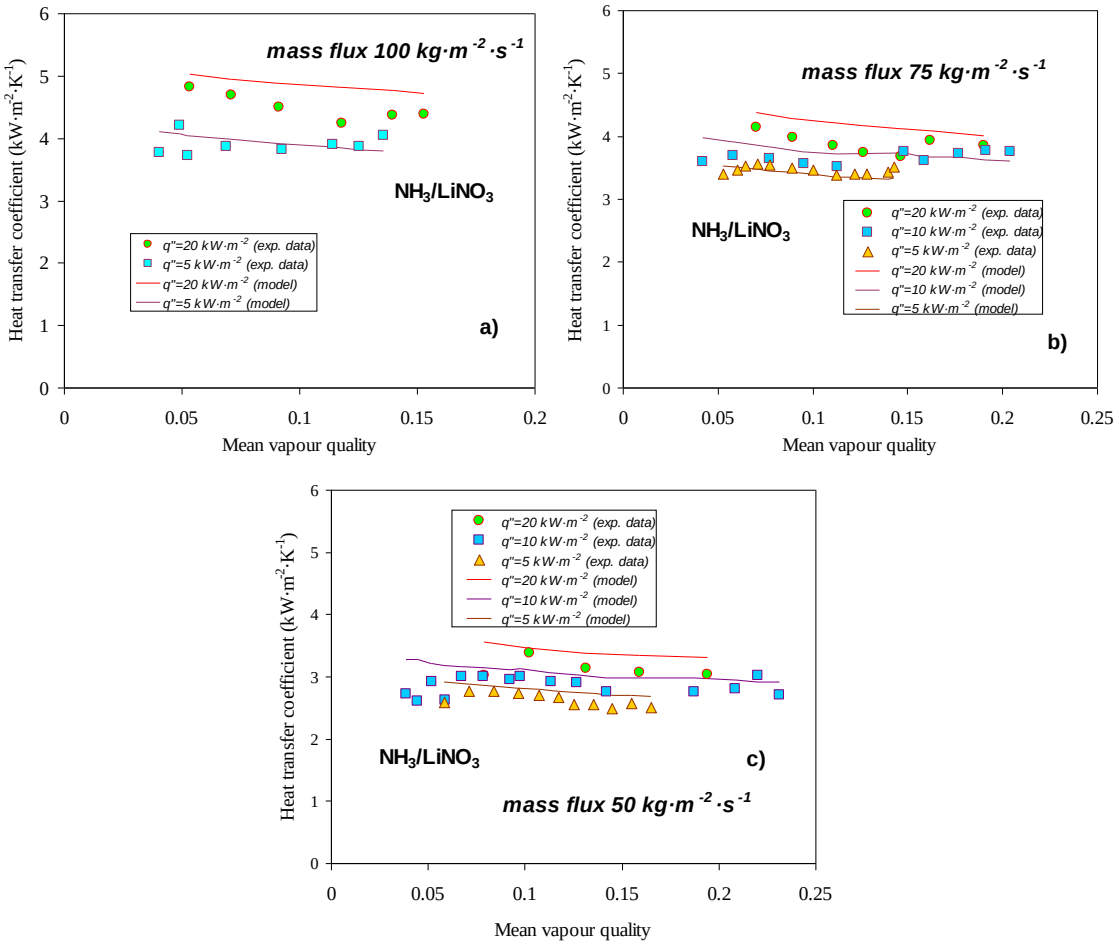

555

556

557 **Figure 12: Comparison between the predicted values by the correlation of Táboas et al. [38] and**
558 **experimental data of the flow boiling heat transfer coefficient for $NH_3/LiNO_3$ at different heat**
559 **fluxes and mass flux of: (a) 100 kg·m^{-2}·s^{-1}, (b) 75 kg·m^{-2}·s^{-1} and (c) 50 kg·m^{-2}·s^{-1}**

560

561 Figure 13 shows a comparison between the experimental flow boiling heat transfer
562 coefficient and the predicted one for both ammonia/lithium nitrate and
563 ammonia/(lithium nitrate + water) fluid mixtures using Eq. (27). Although the
564 experimental data presented for the ternary fluid mixture are scarce, the comparison
565 shows that most of the experimental values are within a maximum deviation from the
566 predicted values of 20%.

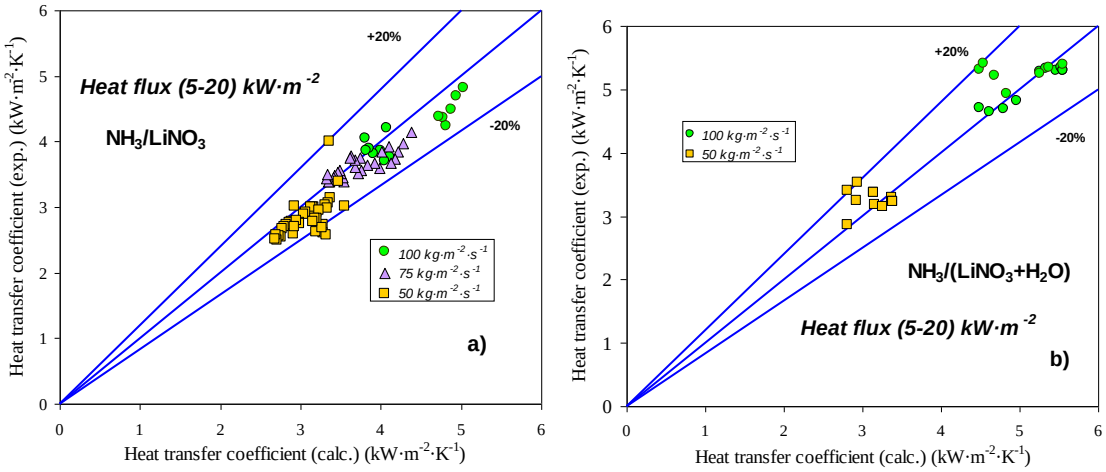

Figure 13: Comparison between the experimental flow boiling heat transfer coefficient and the predicted one using Eq. (27) for: (a) $NH_3/LiNO_3$ and (b) $NH_3/(LiNO_3+H_2O)$

5 Conclusions

Experimental results on flow boiling heat transfer and two-phase pressure drop of ammonia/lithium nitrate and ammonia/(lithium nitrate + water) fluid mixtures in a plate heat exchanger are presented. The experiments were carried out adhering to the operating conditions of absorption equipment for HVAC applications. The effect of mass flux and heat flux on the flow boiling heat transfer coefficient and in the two-phase frictional pressure drop were analysed at vapour qualities ranging from 0 to 0.20. The solution mass flux was varied between 50 and 100 $kg \cdot s^{-1} \cdot m^{-2}$ and the heat flux between 7.5 and 20 $kW \cdot m^{-2}$.

The major conclusions are summarized in the following paragraph:

- The solution mass flux is the parameter that most influences the flow boiling coefficient at the applied operating conditions. This is characteristic of convective boiling. This trend, observed mainly for low heat fluxes and high solution mass

fluxes, showed that the boiling coefficient improves when the solution mass flux is increased.

- For the binary fluid mixture of ammonia/lithium nitrate the increase of the flow boiling coefficient, is more significant at low values of heat flux, when the mass flux is increased. However, with the ternary fluid mixture of ammonia/(lithium nitrate + water) the improvement of the flow boiling coefficient, achieved by increasing the solution mass flux, is similar for all the values considered for heat flux.
- For the ternary fluid mixture of ammonia/(lithium nitrate + water) the flow boiling coefficient was not influenced by the heat flux variation. It indicated a predominance of convective boiling at the operating conditions applied, and as in the case of the binary fluid mixture, the effect of vapour quality on the flow boiling coefficient was almost insignificant.
- The frictional two-phase pressure drop in the plate heat exchanger (PHE) increased almost linearly with the mean vapour quality. The vapour quality followed by the mass flux had the most influence on the frictional two-phase pressure drop in the PHE. The influence of the heat flux on the frictional pressure drop was almost insignificant.
- The Chisholm correlation with the constant C=3 obtained by Táboas et al. [38], can satisfactorily predict the two-phase pressure drop in a plate heat exchanger (PHE).
- The correlation of Táboas et al. [38] initially proposed for ammonia/water in the PHE, can satisfactorily predict the flow boiling heat transfer coefficient for ammonia/lithium nitrate and ammonia/(lithium nitrate + water) fluid mixtures.

608 # Acknowledgement

609 This study is part of an R&D project funded by the Spanish Ministry of Science and
610 Innovation (ENE2008-00863).

611

612

References

1. Táboas, F., M. Vallès, M. Bourouis, and A. Coronas, *Flow boiling heat transfer of ammonia/water mixture in a plate heat exchanger.* International Journal of Refrigeration, 2010. 33(4): p. 695-705.
2. Gensch, K., *Lithiumnitratammoniakat als absorptionsflüssigkeit für kältemaschinen.* Zietschr. Kälte-Ind., 1937. 1(2).
3. Aggarwal, M.K. and R.S. Agarwal, *Thermodynamic properties of lithium nitrate-ammonia mixtures.* International Journal of Energy Research, 1986. 10(1): p. 59-68.
4. Infante Ferreira, C.A., *Thermodynamic and physical property data equations for ammonia-lithium nitrate and ammonia-sodium thiocyanate solutions.* Solar Energy, 1984. 32(2): p. 231-236.
5. Antonopoulos, K.A. and E.D. Rogdakis, *Performance of solar-driven ammonia-lithium nitrate and ammonia--sodium thiocyanate absorption systems operating as coolers or heat pumps in Athens.* Applied Thermal Engineering, 1996. 16(2): p. 127-147.
6. Kim, D.S. and C.H.M. Machielsen, *Comparative study on water- and air-cooled solar absorption chillers*. in *EuroSun 2002 ISES Conference*. 2002. Bologna, Italy.
7. Niebergall, W., *Arbeitsstoffpaare für Absorptions-Kältean- lagen und Absorptions-Kuhlschranke.* Markewitz-Verlag G.M.B.H: Darmstandt, 1949.
8. Sun, D.W., *Comparison of the performances of NH_3-H_2O, NH_3-$LiNO_3$ and NH_3-NaSCN absorption refrigeration systems.* Energy Conversion and Management, 1998. 39(5-6): p. 357-368.
9. Bourouis, M., M. Vallès, and A. Coronas. *Absorption refrigeration cycles driven by thermal energy at low temperature*. In *Eurotherm Seminar No. 72*. 2003.
10. Arzoz, D., M.d. Venegas, P.A. Rodríguez, and M. Izquierdo. *Solar absorption refrigeration cycle using $LiNO_3$-NH_3 solution and flat plate collectors, ISHPC'02,*

    Proc. Of the Int. , Shangai, China, 2002. in *International Sorption Heat Pump Conference*. 2002. Shangai.
11. Ayala, R., C.L. Heard, and F.A. Holland, *Ammonia/lithium nitrate absorption/compression refrigeration cycle. Part I. Simulation.* Applied Thermal Engineering, 1997. 17(3): p. 223-233.
12. Ayala, R., J.L. Frías, L. Lam, C.L. Heard, and F.A. Holland, *Experimental assessment of an ammonia/lithium nitrate absorption cooler operated on low*

temperature geothermal energy. Heat Recovery Systems and CHP, 1994. 14(4): p. 437-446.

13. Infante Ferreira, C.A. *Operating characteristics of NH_3-$LiNO_3$ and NH_3-NaSCN absorption refrigeration machines.* In *19th International Congress of Refrigeration*. 1995.

14. Heard, C.L., Ayala, R. and Best, R., . *An experimental comparison of an absorption refrigerator using ammonia/water and ammonia/lithium nitrate*. in *International Absorption Heat Pump Conference*. 1996. Montreal, Canada.

15. Ehmke, H.J. and M. Renz. *Ternary Working Fluids for Absorption Systems with Salt-Liquid Mixtures as Absorber*. In *IIF - IIR Congress, Commission B1,, 1983.* 1983. Paris, France.

16. Bokelmann, H., H.J. Ehmke, and F. Steimle. *Presentation of New Working Fluids for Absorption Heat Pumps*. In *Absorption Experts Meeting*. 1985. Paris, France.

17. Reiner, R.H. and A. Zaltash, *Evaluation of ternary ammonia-water fluids for GAX and regeneration absorption cycles*. 1991.

18. Manago, A., *ANNEX 14, Working Fluids and Transport Phenomena in Advanced Absorption Heat Pumps,* in *Research and Development on Working Fluids*. 1995.

19. Bothe, A., *Das Stoffsystem NH3---$LiNO_3$/H_2O für den Einsatz in Absorptionskreisläufen*. 1989, Universität Essen Duisburg.

20. Libotean, S., A. Martín, D. Salavera, M. Valles, X. Esteve, and A. Coronas, *Densities, viscosities, and heat capacities of ammonia + lithium nitrate and ammonia + lithium nitrate + water solutions between (293.15 and 353.15) K.* Journal of Chemical and Engineering Data, 2008. 53(10): p. 2383-2388.

21. Libotean, S., D. Salavera, M. Valles, X. Esteve, and A. Coronas, *Vapor-liquid equilibrium of ammonia + lithium nitrate + water and ammonia + lithium nitrate solutions from (293.15 to 353.15) K.* Journal of Chemical and Engineering Data, 2007. 52(3): p. 1050-1055.

22. Linke, W.F., *Solubilities, inorganic and metalorganic compounds : a compilation of solubility data from the periodical literature*. 4th ed, ed. A. Seidell. 1965, Princeton, N.J. : Van Nostrand.

23. Eysseltova, J. and V.T. Orlova, *IUPAC-NIST Solubility Data Series. 89. Alkali Metal Nitrates. Part 1. Lithium Nitrate.* Journal of Physical and Chemical Reference Data, 2010. 39(3): p. 033104-39.

24. Rivera, W. and R. Best, *Boiling heat transfer coefficients inside a vertical smooth tube for water/ammonia and ammonia/lithium nitrate mixtures.* International Journal of Heat and Mass Transfer, 1999. 42(5): p. 905-921.

687 25. Zacarías, A., R. Ventas, M. Venegas, and A. Lecuona, *Boiling heat transfer and*
688 *pressure drop of ammonia-lithium nitrate solution in a plate generator*.
689 International Journal of Heat and Mass Transfer, 2010. 53(21-22): p. 4768-4779.
690 26. Sathyabhma, A. and T.P. Ashok Babu, *Experimental investigation of pool*
691 *boiling heat transfer in ammonia-water-lithium nitrate solution*. Experimental
692 Heat Transfer, 2012. 25 (2), pp. 127-138
693 27. Haltenberger, W., *Enthalpy-Concentration Charts from Vapor Pressure Data*.
694 Industrial & Engineering Chemistry, 1939. 31(6): p. 783-786.
695 28. McNeely, L.A., *Thermodynamic properties of aqueous solutions of lithium*
696 *bromide*. ASHRAE Trans, 1979. 85(pt 1): p. 413-434.
697 29. Cuenca, Y., Salavera, D., Vernet, A., Teja, A.S., Vallès, M. *Thermal*
698 *conductivity of ammonia + lithium nitrate and ammonia + lithium nitrate +*
699 *water solutions over a wide range of concentrations and temperatures*,
700 International Journal of Refrigeration, 2014, 38, p. 333-340.
701 30. Shah, R.K. and W.W. Focke, *Heat transfer equipment desing*. 1988, Washington
702 DC: Hemisphere.
703 31. Hsieh, Y.Y. and T.F. Lin, *Saturated flow boiling heat transfer and pressure*
704 *drop of refrigerant R-410A in a vertical plate heat exchanger*. International
705 Journal of Heat and Mass Transfer, 2002. 45(5): p. 1033-1044.
706 32. Yan, Y. and T. Lin, *Evaporation heat transfer and pressure drop of refrigerant*
707 *R-134a in a plate heat exchanger*. Journal of Heat Transfer-Transactions of the
708 Asme, 1999. 121(1): p. 118-127.
709 33. Claesson, J., *Thermal and Hydraulic performance of compact brazed plate heat*
710 *exchangers operating as evaporators in domestic heat pumps*. 2004, KTH
711 (Royal institute of technology): Stockholm. p. 252.
712 34. Longo, G.A. and A. Gasparella, *Heat transfer and pressure drop during HFC*
713 *refrigerant vaporisation inside a brazed plate heat exchanger*. International
714 Journal of Heat and Mass Transfer, 2007. 50(25-26): p. 5194-5203.
715 35. Palm, B. and J. Claesson, *Plate heat exchangers: Calculation methods for*
716 *single-and two-phase flow*. Heat Transfer Engineering, 2006. 27(4): p. 88-98.
717 36 Han, D. H., K. J. Lee y Y. H. Kim, *Experiments on the characteristics of*
718 *evaporation of R410A in brazed plate heat exchangers with different geometric*
719 *configurations*. Applied Thermal Engineering, 2003. 23(10): p. 1209-1225.
720 37. Djordjevic, E., Kabelac, S., *Flow boiling of R134a and ammonia in a plate heat*
721 *exchanger*. International Journal of Heat and Mass Transfer, 2008. 51(25-26): p.
722 1033-1044.

38. Táboas, F., M. Vallès, M. Bourouis, and A. Coronas, *Assessment of boiling heat transfer and pressure drop correlations of ammonia/water mixture in a plate heat exchanger.* International Journal of Refrigeration, 2012. 35(3): p. 633-644.

Figures caption

Figure 1: Schematic diagram of the experimental test bench

Figure 2: Main parameters of the plate heat exchanger

Figure 3: Two-phase pressure drop versus mean vapour quality at different mass fluxes and heat fluxes for: (a) $NH_3/LiNO_3$ and (b) $NH_3/(LiNO_3+H_2O)$

Figure 4: Two-phase friction factor versus mean vapour quality at different mass fluxes and heat fluxes for: (a) $NH_3/LiNO_3$ and (b) $NH_3/(LiNO_3+H_2O)$

Figure 5: Flow boiling heat transfer coefficient versus mean vapour quality for $NH_3/LiNO_3$ at different mass fluxes and heat flux of: (a) 5 $kW \cdot m^{-2}$, (b) 10 $kW \cdot m^{-2}$ and (c) 20 $kW \cdot m^{-2}$

Figure 6: Flow boiling heat transfer coefficient versus mean vapour quality for $NH_3/LiNO_3$ at different heat fluxes and mass flux of: (a) 100 $kg \cdot m^{-2}s^{-1}$, (b) 75 $kg \cdot m^{-2}s^{-1}$ and (c) 50 $kg \cdot m^{-2}s^{-1}$

Figure 7: Comparison between the flow boiling heat transfer coefficients of the binary and ternary fluid mixtures at: (a) heat flux of 20 $kW \cdot m^{-2}$ and mass flux of 100 $kg \cdot m^{-2} \cdot s^{-1}$; (b) heat flux of 10 $kW \cdot m^{-2}$ and mass flux of 50 $kg \cdot m^{-2} \cdot s^{-1}$

Figure 8: Comparison of the flow boiling heat transfer coefficient with $NH_3/LiNO_3$ fluid mixture (present work) with data obtained by Táboas et al. [1] for NH_3/H_2O

Figure 9: Two-phase frictional pressure drop for: (a) binary and ternary fluid mixtures, (b) binary, ternary and NH_3/H_2O fluid mixtures

Figure 10: Frictional pressure drop per unit length versus the kinetic energy per unit volume. Comparison between the present work and Zacarías et al. [25].

Figure 11: Comparison between the predicted values by the correlation of Táboas et al. [38] and experimental data of the flow boiling heat transfer coefficient for $NH_3/LiNO_3$ at different mass fluxes and heat flux of: (a) 5 $kW \cdot m^{-2}$, (b) 10 $kW \cdot m^{-2}$ and (c) 20 $kW \cdot m^{-2}$

Figure 12: Comparison between the predicted values by the correlation of Táboas et al. [38] and experimental data of the flow boiling heat transfer coefficient for $NH_3/LiNO_3$

757 at different heat fluxes and mass flux of: (a) 100 $kg \cdot m^{-2} \cdot s^{-1}$, (b) 75 $kg \cdot m^{-2} \cdot s^{-1}$ and (c) 50
758 $kg \cdot m^{-2} \cdot s^{-1}$

759 Figure 13: Comparison between the experimental flow boiling heat transfer coefficient
760 and the predicted one using Eq. (27) for: (a) $NH_3/LiNO_3$ and (b) $NH_3/(LiNO_3+H_2O)$

761

762

763 **Tables caption**

764 Table 1: Accuracy of measured variables and combined uncertainty of the calculated
765 parameters

766 Table 2: Operating conditions

767